Anaerobic ammonium oxidation (anammox) and denitrification in Peru margin sediments

Jeremy J. Rich[a,*], Philip Arevalo[b], Bonnie X. Chang[c], Allan H. Devol[d], Bess B. Ward[e]

[a] *School of Marine Sciences and Darling Marine Center, University of Maine, Walpole, ME, 04573, USA*
[b] *Department of Ecology & Evolution, University of Chicago, Chicago, IL, 60637, USA*
[c] *Joint Institute for the Study of the Atmosphere and Ocean, University of Washington, NOAA/Pacific Marine Environmental Laboratory, Seattle, WA, 98115*
[d] *School of Oceanography, University of Washington, Seattle, WA, 98195, USA*
[e] *Department of Geosciences, Princeton University, Princeton, NJ, 08544, USA*

ABSTRACT

The upwelling system of coastal Peru supports very high primary production, contributing to an oxygen deficient zone (ODZ) in subsurface waters and high organic matter deposition rates to underlying sediments. Although anammox and denitrification have been relatively well studied in ODZ waters, few studies have investigated these processes in the underlying sediments. We sampled seven stations over a large geographic area along the Peru margin, spanning a water depth of 100–3240 m. At two of the central shelf stations (100 m and 325 m), we observed *Thioploca*, with a well-developed mat at the shallowest station (100 m). We measured sediment properties and conducted shipboard ^{15}N-incubations of homogenized sediments to determine potential rates of anammox and denitrification and potential controlling factors at each station. Diversity of anammox bacteria based on 16S rRNA and hydrazine oxidoreductase (*hzo*) sequences and *hzo* gene abundances were measured at each station. Overall, organic C content was high across the stations (3–12%), except for two of the deepest stations (~1.5%). Porewater ammonium fluxes and ammonium production rates in shipboard incubations, reflecting sediment organic carbon decomposition rates, were higher at the two central shelf stations compared to the other stations. The range in average potential rates was 2.1–80.4 nmol N cm^{-3} h^{-1} for denitrification and 1.8–44.2 nmol N cm^{-3} h^{-1} for anammox. The range in relative anammox (*ra*) across stations was 2.6–47.4%, with an average of 34.2%. The lowest *ra* was found at the shallowest shelf station with *Thioploca* mats and highest ammonium production rates. The *ra* jumped up to 45.9% at the station with the next highest ammonium production rates, corresponding to the deeper shelf station (325 m). At the other stations, *ra* was relatively high (39.6–47.4%), except at one station (16.3%), reflecting similar ammonium production rates due to decomposition across these stations. Anammox bacteria in the *Candidatus* Scalindua genus were the only anammox bacteria detected in Peru margin sediments based on 16S rRNA or *hzo* sequences. Copy number of *hzo* indicated abundant populations of anammox bacteria across the stations. However, *hzo* copy number did not correlate with anammox rates or *ra*. Overall, our results suggest that anammox contributes significantly to N$_2$ production in Peru margin sediments, except in shelf sediments with high decomposition rates and dense *Thioploca* mats.

1. Introduction

Nitrogen is the macronutrient most often limiting primary productivity in marine ecosystems. Therefore, processes that control the fate and abundance of nitrogen are critical to ecosystem functioning. Denitrification is the step-wise reduction of NO$_3^-$ to N$_2$, coupled to the oxidation of organic carbon, H$_2$, reduced sulfur, or ferrous iron, under anoxic conditions. Denitrification is carried out by a diverse polyphyletic group of bacteria and some archaea, including phototrophic, chemolithotrophic, and heterotrophic organisms and even eukaryotes, such as foraminifera (Risgaard-Petersen et al., 2006; Zumft, 1997). Anaerobic ammonium oxidation (anammox) is the oxidation of NH$_4^+$, with NO$_2^-$, in the absence of O$_2$ to form N$_2$. Anammox is carried out by a monophyletic group of *Planctomycetes*. Although anammox bacteria can oxidize organic acids, they grow primarily as autotrophs (Kartal et al., 2011a). It has long been assumed that denitrification was the

dominant process producing N$_2$ under anoxic conditions in natural ecosystems. It is now clear, however, that anammox is an important alternative pathway of N$_2$ production in the global nitrogen cycle. Information regarding the relationship between anammox and denitrification in terms of N$_2$ production is critical for understanding the global nitrogen cycle.

An important sink in global N budgets occurs in the water column of the major oxygen deficient zones (ODZs), located in the Eastern Tropical North and South Pacific and in the Arabian Sea (Galloway et al., 2004). The relative contribution of anammox and denitrification to N$_2$ flux in these regions has received considerable attention, and either anammox or denitrification contributes substantially to N$_2$ production, depending on timing and location, while overall the contribution of anammox is likely to be limited by stoichiometric constraints (Dalsgaard et al., 2012; Lam et al., 2009; Ward et al., 2009; Babbin et al., 2014). However, uncertainties about which process

---

dominates at any given location or time, indicate that factors controlling the relative contribution of each process are still not adequately understood. An even larger N sink occurs in ocean sediments, particularly continental shelf and slope sediments, and possibly deep-sea sediments. A number of studies of denitrification in marine sediments exist, especially in shelf sediments, and denitrification has been modeled in deep-sea sediments (e.g., Christensen et al., 1987; Devol, 1991, and Middelburg et al., 1996). Thamdrup and Dalsgaard (2002) first demonstrated that anammox accounted for up to 67% of N_2 production in sediments from the Skagerrak, with the remaining N_2 resulting from denitrification. The experiments conducted by Thamdrup and Dalsgaard (2002) were based on incubations of homogenized sediments amended with $^{15}NO_3^-$ and are generally referred to as isotope pairing experiments, building off earlier work (Nielsen, 1992). The relative contribution of anammox to the total N_2 production rate in these types of incubations is referred to as ra (i.e., $ra = 100[$(anammox rate) / (anammox rate + denitrification rate)]; Trimmer and Engström, 2011). Engström et al. (2005) found somewhat higher ra (79%) at some of the same sites sampled by Thamdrup and Dalsgaard (2002) in the Skagerrek. In both studies, ra increased with depth due to lower rates of denitrification linked to lower rates of overall organic C decomposition rates with water depth, while anammox rates were relatively more constant than denitrification rates. This suggested that flux of labile organic carbon was one of the primary factors controlling ra, as driven primarily by changes in rates of denitrification rather than anammox. Since the original work in the Skagerrak, many more studies have measured anammox and denitrification potential rates, confirming that ra is generally low in shallow coastal sediments (Trimmer and Engström, 2011). Measurements in deep-sea sediments are less common, but the measurements that have been made confirm that ra is higher in deeper sediments compared to coastal sediments, although there are exceptions (Trimmer and Nicholls, 2009; Engström et al., 2009, and Sokoll et al., 2012).

At least five genera of anammox bacteria have been identified thus far, including *Candidatus* Brocadia, Kuenenia, and Scalindua, which together form a deeply branching group of *Planctomycetes,* based on 16S rRNA gene sequences (Kartal et al., 2011a). A variety of environments have been examined for 16S rRNA genes specific for anammox bacteria, and Ca. Scalindua is the only genus usually detected in marine environments (Sonthiphand et al., 2014). Hydrazine is an intermediate in the anammox reaction, and hydrazine oxidoreductase (Hzo) has been identified as a key enzyme in the pathway, oxidizing hydrazine to N_2 (Kartal et al., 2011b). Hzo is in the octaheme cytochrome hydroxylamine oxidoreductase (Hao) family of proteins, of which several divergent octaheme protein coding sequences are found in anammox bacteria. In the Kuenenia genome, there are two copies of nearly identical Hzo sequences corresponding to functional proteins responsible for hydrazine oxidation to N_2. These two protein sequences form a specific phylogenetic cluster distinct from other putative Hzo/ Hao proteins (Kartal and Keltjens, 2016; Klotz et al., 2008; Schmid et al., 2008). PCR primers have been developed to detect the gene sequences corresponding to the two functional Hzo proteins, thereby serving as a biomarker of anammox bacteria in the environment (Hirsch et al., 2011; Schmid et al., 2008).

The water column off Peru is characterized by high primary productivity and a large ODZ, with high rates of organic matter deposition to underlying sediments (Froelich et al., 1988; Hedges and Keil, 1995; Henrichs and Farrington, 1984; Levin et al., 2002). The Peruvian ODZ occurs at water depth of ~20–500 m. As such, shelf sediments are covered by anoxic water conducive to the growth of *Thioploca* bacteria that can form thick fibrous mats at certain locations (Fossing et al., 1995; Schulz et al., 1996). *Thioploca* store up to 550 mM NO_3^- in internal vacuoles and they respire NO_3^- to NH_4^+, rather than N_2, in the process known as dissimilatory nitrate reduction to ammonium (DNRA), with reduced sulfur as an electron donor (Otte et al., 1999). Anammox bacteria have been shown to form specific associations with

Thioploca filaments, as *Thioploca* can produce both substrates needed in the anammox reaction (Prokopenko et al., 2013). However, based on simulation models of measured solute fluxes, anammox rates were relatively low compared to denitrification in sediments with *Thioploca* mats on the Peruvian shelf (Bohlen et al., 2011). Furthermore, foraminifera contain very high concentrations of intracellular NO_3^-, as well, and could theoretically account for a significant portion of denitrification in Peru margin sediments (Glock et al., 2013). Release or mixing of intracellular $^{14}NO_3^-$ from *Thioploca* or foraminifera in sediment incubations with added $^{15}NO_3^-$ has the potential to lead to significant overestimates of anammox rates, if intracellular $^{14}NO_3^-$ is not adequately accounted for (Sokoll et al., 2012 and Song et al., 2013). DNRA produces $^{15}NH_4^+$ from added $^{15}NO_3^-$ that can then combine with $^{15}NO_2^-$, leading to an underestimate of anammox rates (Song et al., 2013 and Song et al., 2016). As significant intracellular NO_3^- and DNRA would be expected to occur at some locations in Peru margin sediments, modifications to the standard isotope pairing method would be necessary to determine anammox and denitrification rates in these situations (Sokoll et al., 2012; Song et al., 2013, and Song et al., 2016).

In the current study, we used the ^{15}N-isotope pairing technique to measure potential rates of anammox and denitrification in homogenized sediments from seven stations in the Peru margin that spanned a water depth of 100–3250 m. We also measured the diversity of anammox specific 16S rRNA and *hzo* sequences, and the abundance of *hzo* genes using quantitative PCR at the same stations. Our objectives were to provide the first direct measurements of anammox and denitrification potential rates in Peru margin sediments using isotope pairing, thereby providing further insights into processes that may regulate anammox in marine sediments and the potential significance of anammox as a nitrogen loss pathway in the Peru margin sediments.

2. Methods

2.1. Sample locations and site characteristics

A multi-corer (Ocean Instruments, MC-800) was used to obtain intact surface sediments at seven stations in the Peru margin, aboard the R/V Knorr in October 2005 (leg 182–9) (Fig. 1, Table 1). Bottom water temperature was measured with the CTD (Sea-Bird Electronics, SBE9) and dissolved O_2 of the water column was measured using a probe (Sea-Bird Electronics, SBE43; detection limit ~2 μM) mounted on the CTD, calibrated with the micro-Winkler technique (Broenkow and Cline, 1969). NO_3^- and NO_2^- in the bottom water were measured with sensitivities of ± 0.1 μM for NO_3^- and ± 0.01 μM for NO_2^- using standard techniques (Braman and Hendrix, 1989; Strickland and Parsons, 1972). The percent of total organic carbon (%TOC) in the top 0–1 cm of sediment collected in one of the multi-core tubes at each station was measured in acidified sediment samples with an elemental analyzer (Carlo Erba Model 1108).

2.2. Potential anammox and denitrification rates

The sediment processing, incubation conditions, ^{15}N additions, and analytical measurements were conducted following previously published methods (Rich et al., 2008; Risgaard-Petersen et al., 2004; Thamdrup and Dalsgaard, 2002). Briefly, where bottom waters contained measureable O_2, the oxygen penetration depth was measured with a Clark type microelectrode. Sediments just below the oxygen penetration depth or the top layer of sediment when cores were collected in the ODZ were sectioned (2 cm depth interval) and immediately transferred to an N_2 flushed glove bag, where the sediment was homogenized and transferred to vials (1.5 ml sediment slurry in 5.9 ml Exetainer vials). The vials were sealed and removed from the glove bag, flushed with He, and pre-incubated for 1–3 h at the incubation temperature of 12 °C, such that rates were obtained at the same temperature across stations. Tracer and carrier solutions were
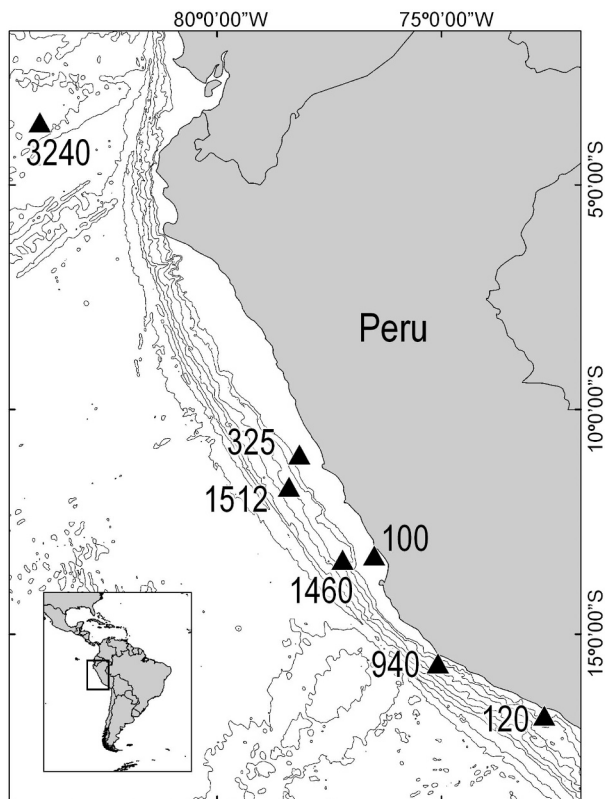
Fig. 1. Location and corresponding water column depth of each station (meters). Bathymetry lines include 500 m and 1000 m isobaths, then 1000 m increments thereafter, down to a depth of 6000 m.

purged with helium and manipulated using helium-purged gas-tight glass syringes. Vials were injected with either $^{15}NO_3^- + ^{14}NH_4^+$, $^{15}NH_4^+$, or $^{14}NO_3^- + ^{15}NH_4^+$ (100 nmol N cm^{-3} sediment) after the preincubation period and triplicate vials were killed at various time points with $ZnCl_2$ (100 µl 7 M) during 8–16 h incubations. The ^{15}N content of the resulting N_2 was determined by isotope ratio mass spectrometry using a Europa 20/20.

In incubations with added $^{15}NO_3^- + ^{14}NH_4^+$, the fraction of $NO_3^- + NO_2^-$ as ^{15}N (F_n) was determined by difference, before and immediately after $^{15}NO_3^-$ addition, accounting for the atom% of the stock solution, except at the two central shelf stations with visible *Thioploca* (100 m and 325 m) (see below). The rates of $^{15}N^{14}N$ and $^{15}N^{15}N$ production from added $^{15}NO_3^-$ and F_n were used in the equations of Thamdrup and Dalsgaard (2002) to calculate potential rates of anammox and denitrification. In incubations that received additions of $^{15}NH_4^+ + ^{14}NO_3^-$, the anammox rate was calculated using the

following equation, as modified from a previous study (Thamdrup and Dalsgaard, 2000): $dN_2/dt = d^{29}N_2/dt \times F_a^{-1}$, where $F_a = (f_0 + f_t)/2$, f_0 = fraction of NH_4^+ that was labeled with ^{15}N at time zero, and f_t = fraction of NH_4^+ that was labeled with ^{15}N at the end of interval t, in which the rate was determined. This was to account for any change in F_a during the course of incubations due to release of $^{14}NH_4^+$ during organic matter decomposition or conversion of added $^{14}NO_3^-$ to $^{14}NH_4^+$ by DNRA. The f_0 was determined by difference, before and immediately after $^{15}NH_4^+$ addition, accounting for the atom% of the stock solution and NH_4^+ in the porewater and adsorbed to sediment colloids, as determined by the recovery of added NH_4^+ in the porewater (Thamdrup and Dalsgaard, 2000). The f_t was calculated according to the following equation: $f_t = ([^{15}NH_{4t0}^+] - 0.5A29)/ (\Sigma NH_{4t}^+)$, where $A29$ is the amount of $^{15}N^{14}N$ produced in the time interval t and ΣNH_{4t}^+ is the measured NH_4^+ concentration at t. Rates were based on difference between the first and second time points as rates leveled off after the second time point in sediment incubations due to complete consumption of added NO_3^- in three of seven stations. In sediments where *Thioploca* sheaths were observed (i.e., 100 m and 325 m), high and variable initial NO_3^- concentrations were measured in unamended sediment slurries, reflecting release of intracellular NO_3^- during sample processing (e.g., Thamdrup and Canfield, 1996). To address this issue, it was assumed that anammox rates in sediments where *Thioploca* sheaths were observe were equivalent in either $^{15}NO_3^- + ^{14}NH_4^+$ or $^{15}NH_4^+ + ^{14}NO_3^-$ additions (Sokoll et al., 2012; Song et al., 2013). This was assumed as anammox rates were equivalent in the two different isotope additions in sediment samples without *Thioploca*. This enabled F_n to be calculated in incubations with added $^{15}NO_3^- + ^{14}NH_4^+$ based on the anammox rate determined in the $^{15}NH_4^+ + ^{14}NO_3^-$ additions and measured $^{15}N^{14}N$ and $^{15}N^{15}N$ production in $^{15}NO_3^- + ^{14}NH_4^+$ additions.

2.3. Porewater depth profiles and ammonium production

Concentration of $NO_3^- + NO_2^-$ and NH_4^+ were measured in porewater depth profiles collected at five of the seven stations using sediment from one of the multi-core tubes at each station. The sediment from the core tube was sectioned in 0.5–1.0 cm intervals, centrifuged, and the supernatant was filtered through 0.45 µm filters (profiles from MC2 and MC9 were not determined). Porewaters were frozen until analyzed for $NO_3^- + NO_2^-$ and NH_4^+ following previously published methods (Koroleff, 1983; analytical error for $NO_3^- + NO_2^-$ was ± 0.1 µM and for NH_4^+ was ± 0.3 µM). A form of Fick's first law was used to calculate the diffusive flux (J) of $NO_3^- + NO_2^-$ and NH_4^+, $J = \phi D_s(\delta_C/\delta z)$, where ($\delta_C/\delta z$) is the steepest measured concentration gradient, ϕ is the porosity, and D_s is the sediment diffusion coefficient. The sediment diffusion coefficient, D_s, was calculated as the product of the molecular diffusion coefficient and the porosity (Ullman and Aller, 1982). The molecular diffusion coefficients of $NO_3^- + NO_2^-$ (D_{nt}) and

Table 1
Multi-core station name, location, water depth, and bottom water characteristics.

Station	Latitude	Longitude	Depth (m)	Temperature (°C)	O_2 (µM)	NO_3^- (µM)	NO_2^- (µM)
Shelf							
MC5	13°15.00′ S	76°30.00′ W	100	13.2	< 2[a]	26.1	2.0
MC2	16°48.83′ S	72°42.88′ W	120	12.3	< 2	ND[b]	ND
MC12	10°60.00′ S	78°10.00′ W	325	10.5	< 2	29.7	1.2
Slope							
MC3	15°38.93′ S	75°04.98′ W	940	4.6	65.1	43.3	< 0.01
MC4	13°20.63′ S	77°12.16′ W	1460	3.2	67.1	41.9	< 0.01
MC9	11°43.05′ S	78°23.93′ W	1512	2.9	71.8	42.4	< 0.01
Rise							
MC15	3°36.23′ S	83°56.88′ W	3240	1.8	112.5	37.1	< 0.01

[a] O_2 concentration was at or below the detection limit of the sensor of ~2 µM.

[b] ND, not determined.

NH_4^+ (D_a) were calculated at the appropriate bottom water temperature using the equations according to Boudreau (1997), $D_{nt} = (9.5 + 0.388\ T)10^{-6}$ and $D_a = (9.5 + 0.413\ T)10^{-6}$, where T is temperature in degrees Celsius.

In the same laboratory incubations that were used to determine anammox and denitrification potential rates, the production rate of dissolved NH_4^+ was determined after NO_3^- was consumed, which would reflect NH_4^+ production from decomposing organic matter as a proxy for flux of labile organic C across sites. As NO_3^- was always present during the incubation from the deepest station (MC15), NH_4^+ loss due to anammox during the incubation was accounted for in the NH_4^+ production rate determined at this station (i.e., $P_a = d[NH_4^+] / dt + 0.5A$, where $P_a = NH_4^+$ production rate, and A = anammox rate).

2.4. Diversity and phylogenetic analyses of anammox specific 16S rRNA and hzo genes

Six sub-samples (0.5 ml) of the homogenized sediment slurry from each station were flash frozen in liquid N_2 and transported back to the laboratory. Total DNA was extracted using the MoBio PowerSoil DNA Isolation kit and quantified on a Qubit Fluorometer (Invitrogen). Extracts were diluted to a final concentration of 10 ng DNA μl^{-1} and duplicate extracts were pooled, resulting in three replicate DNA extracts per site. The *Planctomycete*-specific primer Pla46 (5′-GGATTAGGCATG CAAGTC-3′) (Neef et al., 1998) and the anammox-specific primer BS820R (5′-TAATTCCCTCTACTTAGTGCCC-3′) (Kuypers et al., 2003) were used to amplify a 807 bp fragment of the 16S rRNA gene (Schmid et al., 2005), and primers hzocl-f1 (5′-TGYAAGACYTGYCAYTGG-3′) and hzocl-r2 (5′-ACTCCAGATRTGCTGACC-3′) were used to amplify a 471 bp fragment of the anammox-specific gene hydrazine oxidor-eductase (*hzo*) (Schmid et al., 2008), using the following reaction conditions: 40 ng template DNA, 0.2 mM dNTP, 0.064% BSA, 0.03 units μl^{-1} GoTaq HotStart Polymerase (Promega), 0.4 μM forward primer, 0.4 μM reverse primer, $1 \times$ GoTaq Flexi Buffer (Promega), and a final reaction volume of 20 μl. After an initial denaturation at 94 °C for 5 min the following cycle was repeated 30 times: denaturation at 94 °C for 60 s, 60 annealing at 56 °C for 60 s, and extension at 72 °C for 90 s. After the final cycle, a 10 min final extension step was performed at 72 °C. PCR products were run on a 1.5% agarose gel and visualized under UV light with 1.5% ethidium bromide. Fragment bands of the appropriate size were excised from gels and the DNA was extracted using the QIAquick Gel Extraction Kit (Qiagen). PCR products were ligated into the pGEM-T vector (Promega) and transformations were performed according to the manufacturer's instructions. Approximately 20 clones with inserts for each gene, from each station, were selected at random for sequencing using the Sanger method (Genetic Analyzer 3500, Applied Biosystems). The *hzo* nucleotide and amino acid sequences were aligned in muscle (Schloss et al., 2009), and the final alignment for amino acid sequences was 145 residues and for nucleotide sequences was 435 bp. The 16S rDNA sequences were aligned in NAST as implemented on the greengenes website, and the final alignment was 768 bp (Desantis et al., 2006). The 16S rDNA operational taxonomic units (OTUs) were grouped at the 98% similarity level, *hzo* nucleotides sequences at the 96% similarity level, and amino acid sequences at the 99% similarity level using the farthest neighbor method as implemented in mothur (Schloss et al., 2009). Maximum-likelihood phylogenetic trees were generated on the PhyML online platform with one hundred bootstrap replicates (Guindon et al., 2010).

2.5. hzo gene abundance

For quantitative PCR, the Primer3 program was used to design suitable forward and reverse primers based on the 112 *hzo* sequences generated in this study, specifying a product of between 100 and 200 bp in length (Rozen and Skaletsky, 1999). The derived forward (hzo-qf; 5′-CACAAGTATGGGTATGTCAAATGC-3′) and reverse (hzo-qr, 5′-TTG CAAACCTTGGTGAATG-3′) primers amplified a 106 bp *hzo* fragment and were a perfect match for 97 of the 112 *hzo* sequences generated in this study, with one or two mismatches for the remaining sequences. Triplicate DNA extracts from each station were subjected to qPCR using the following conditions: $1\times$ Phusion Flash enzyme master mix (Finnzymes), $1\times$ SYBR green (Invitrogen), 0.5 μM forward primer, 0.5 μM reverse primer, 2 ng template DNA, and a final reaction volume of 20 μl. Reactions were performed on TwinTec Realtime 96-well white PCR plates on the Mastercycler Realplex thermal cycler (Eppendorf). After an initial 10 s denaturation step at 98 °C, the following cycle was repeated 40 times: 98 °C denaturation for 1 s, 58 °C annealing for 5 s, and 72 °C extension for 8 s with a hold for plate reading. Linearized plasmids containing a known copy number of *hzo* were used to generate standard curves.

2.6. Accession numbers

Gene sequences were submitted to Genbank on under accession numbers JQ308954-JQ309035 for 16S rRNA and AFF59692-AFF59803 for *hzo*.

3. Results

3.1. Station and sediment characteristics

The sample locations were distributed over a broad area along the Peru margin, spanning a water depth of 100–3240 m (Fig. 1, Table 1). There was one shelf station along the thin shelf section of southern Peru and two shelf stations in the broader shelf area of central Peru, with O_2 concentrations in the bottom water at or below the detection limit and high NO_2^- concentrations. The three slope stations were in the central or southern areas of the study region and had an O_2 concentration of 65–72 μM in the overlying water. The rise station was off northern Peru and had an O_2 concentration of 112 μM in the overlying water. Since O_2 at the shelf stations was at or below detection, oxygen penetration depth in these sediments was not measured. The range in O_2 penetration in slope sediments was 0.5–0.8 cm, while O_2 penetration at the rise station was 1.5 cm (Table 2). Across stations, the range in %TOC was 1.5–12.5%, with the highest %TOC (> 7%) at the two central shelf stations and one of the slope stations. At the two central shelf stations, *Thioploca* was visually observed in multi-cores, with a dense mat of *Thioploca* at the shallowest station, 100 m, and low density *Thioploca* mat with sparse filaments at 325 m.

3.2. Porewater depth profiles

$NO_3^- + NO_2^-$ concentrations were significantly higher in the porewater of surface sediments of the central shelf stations, reflecting release of intracellular NO_3^- during centrifugation of sediment slices, presumably due to disturbance of *Thioploca* during sample processing (Fig. 2) Meanwhile $NO_3^- + NO_2^-$ profiles for the slope and rise stations did not appear influenced by any release of intracellular NO_3^-, and downward $NO_3^- + NO_2^-$ fluxes at these stations were determined based on porewater profiles (Table 2). The porewater NH_4^+ concentration was higher in surface sediments at the central shelf stations compared to the slope and rise stations, and had correspondingly higher upward NH_4^+ fluxes. There was a slight increase in NH_4^+ in the surface layer at 940 m and 3240 m stations, presumably reflecting cell lysis during core retrieval in the surface layer of these sediments (Berelson et al., 1990; Haeckel et al., 2001), which overall had lower NH_4^+ concentrations throughout the profile. The increase in surface NH_4^+ should not influence calculated NH_4^+ fluxes as the flux calculations are based on the steepest gradient below the surface increase in NH_4^+. Downward $NO_3^- + NO_2^-$ fluxes were higher than upward NH_4^+ fluxes at the three stations where it was possible to make a comparison. At these three stations, assuming that all of the upward NH_4^+ flux was

Table 2

Multi-core sediment characteristics. The $NO_3^- + NO_2^-$ flux is downward and NH_4^+ flux is upward based on porewater depth profiles.

Station	Depth (m)	*Thioploca* mat	O_2 penetration depth (cm)	%TOC	$NO_3^- + NO_2^-$ flux (mmol m^{-2} d^{-1})	NH_4^+ flux (mmol m^{-2} d^{-1})	Porewater flux *ra* (%)[c]
Shelf							
MC5	100	Yes	ND[a]	7.5	NC[b]	1.031	ND
MC2	120	No	ND	3.0	ND	ND	ND
MC12	325	Sparse	ND	12.5	NC	0.638	ND
Slope							
MC3	940	No	0.5	4.3	0.672	0.043	12.1
MC4	1460	No	0.7	7.6	0.499	0.141	44.0
MC9	1512	No	0.8	1.5	ND	ND	ND
Rise							
MC15	3240	No	1.5	1.7	0.148	0.029	32.9

[a] ND = Not determined.

[b] NC = Not calculated because of intracellular nitrate release during core slicing and centrifugation.

[c] This is the relative anammox rate based on porewater fluxes, $ra = 100(2A / (A + N))$, where A is upward NH_4^+ flux and N is the downward NO_3^- flux.

consumed by anammox, and all of the downward flux of $NO_3^- + NO_2^-$ was converted to N_2 either by denitrification or anammox, the range in percent of N_2 production attributed to anammox was 12–44% (Table 2). Note that this calculation does not take into account the possibility of nitrification occurring at very low O_2 concentrations (Bristow et al., 2016).

3.3. ^{15}N-sediment incubations

When NO_3^- or NO_2^- disappeared in incubations of homogenized sediments, $^{15}N-N_2$ production ceased (Figs. 3 and 4). $^{15}N^{14}N$ production exceeded or was similar to that of $^{15}N^{15}N$ in sediments with added $^{15}NO_3^- + ^{14}NH_4^+$, except 940 m where $^{15}N^{15}N$ was higher than $^{15}N^{14}N$ production (second from top row, Figs. 3 and 4). In sediments with added $^{15}NH_4^+$ only or $^{15}NH_4^+ + ^{14}NO_3^-$, $^{15}N^{15}N$ production was not detected in any of the sediments (bottom two rows, Figs. 3 and 4).

In sediments with added $^{15}NH_4^+ + ^{14}NO_3^-$, significant $^{15}N^{14}N$ production was detected in all the sediments, except 100 m (bottom row, Figs. 3 and 4). The total accumulation of $^{15}N^{14}N$ was higher in sediments with added $^{15}NH_4^+ + ^{14}NO_3^-$ than in sediments with added $^{15}NH_4^+$ only, except in 100 m station samples where $^{15}N^{14}N$ was very low or not detected in either treatment (compare bottom two rows, Figs. 3 and 4). $^{15}N^{14}N$ production in the presence of $^{15}NH_4^+$ alone reflected the concentration of $NO_3^- + NO_2^-$ that was present in the vials at the end of 1–3 h preincubations and levels of anammox rates in samples. At the 100 m station there was ~100 nmol N cm^{-3} of $NO_3^- + NO_2^-$ present after the pre-incubation step but very low or no production of $^{15}N^{14}N$ in either $^{15}NH_4^+ + ^{14}NO_3^-$ or $^{15}NH_4^+$ only treatments, indicating low anammox rates at the 100 m station. In samples from the 940 m station there was the lowest concentration of $NO_3^- + NO_2^-$ present (< 1 nmol N cm^{-3}) after the preincubation step and $^{15}N^{14}N$ production was not detected in these
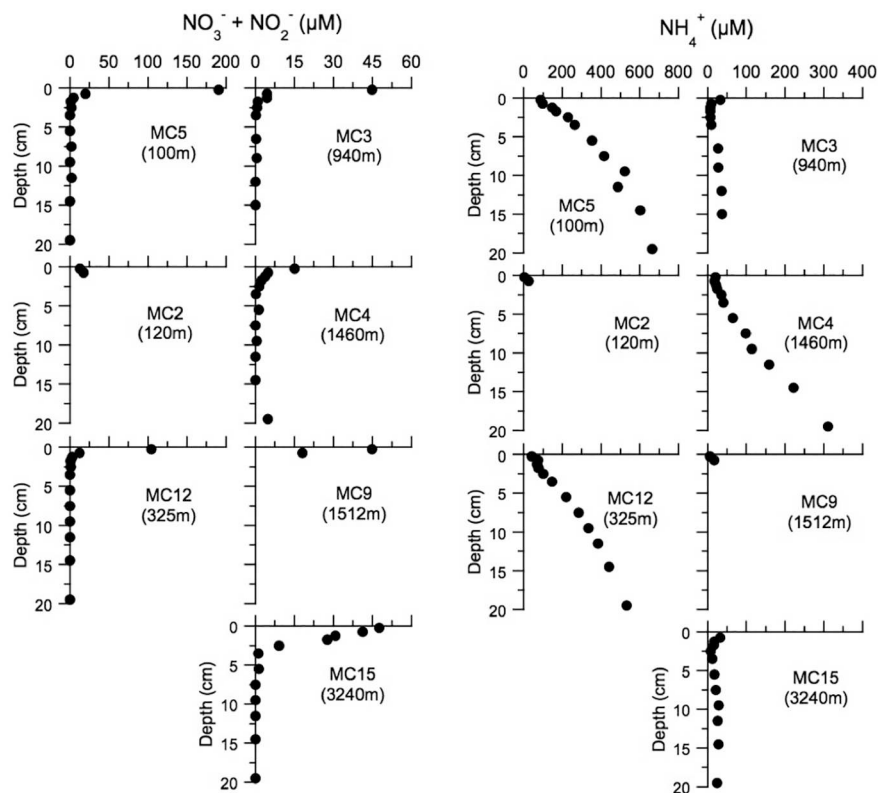

Fig. 2. Porewater depth profiles of $NO_3^- + NO_2^-$ and NH_4^+ concentrations at the multi-core stations [note: Profiles were not measured at stations MC2 (125 m) and MC9 (1512 m). There are different scales for $NO_3^- + NO_2^-$ and NH_4^+, corresponding to higher concentrations at the two shelf stations (MC5 and MC12).
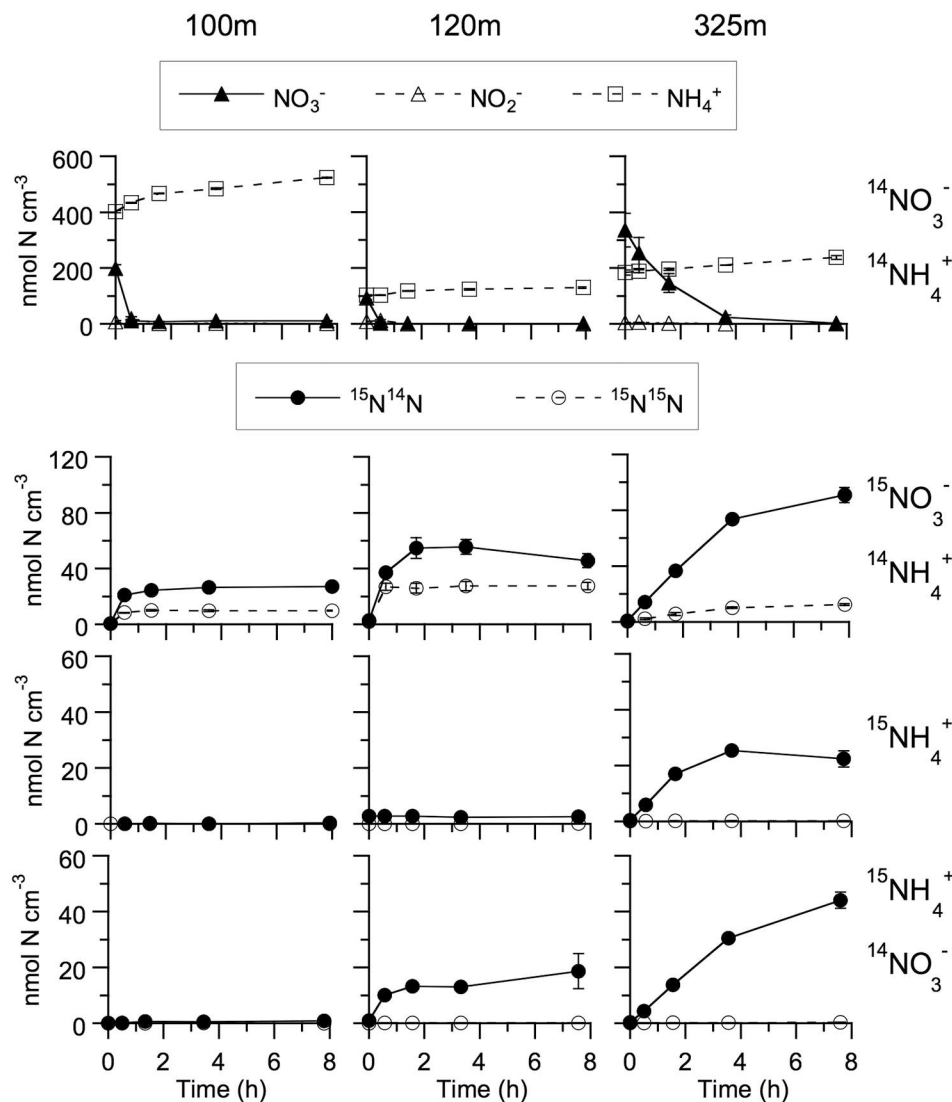
Fig. 3. Dissolved inorganic N and $^{15}N-N_2$ production in incubations of homogenized sediments from the Peru margin shelf stations. Concentrations of NO_3^-, NO_2^-, and dissolved NH_4^+ in the porewater of sediments with added NO_3^- and NH_4^+ (top row), and production of $^{15}N-N_2$ in sediments with different combinations of added $^{14/15}N$ (bottom three rows) are shown (average $\pm$ SE, $n = 3$). The panels are organized in columns, one column for each station (identified by depth), and rows, one row for each N addition (identified at right). Note that the scale for nmol N cm^{-3} differs among rows.

samples with added $^{15}NH_4^+$ only.

There was significant release of intracellular NO_3^- in incubations with sediments from the central shelf stations (100 m and 325 m stations). Therefore, we relied on only one of the isotope additions (i.e., $^{15}NH_4^+ + {}^{14}NO_3^-$ additions) to determine anammox rates at the 100 m and 325 m stations. At the other five stations, we were able to determine anammox rates based on either isotope addition (i.e., $^{15}NH_4^+ + {}^{14}NO_3^-$ and $^{15}NO_3^- + {}^{14}NH_4^+$). At these five stations, there was agreement in anammox rates between the two combinations of isotope additions, with a positive correlation and slope not significantly different from one across five stations (Fig. 5).

The range in average rates across stations was 1.8–44.2 nmol N cm^{-3} h^{-1} for anammox and 2.1–80.4 nmol N cm^{-3} h^{-1} for denitrification (Table 3, Fig. 6C). Except for the shallowest station (100 m), anammox potential rates decreased with depth. Denitrification potential rates also decreased with depth, with the exception of the 930 m station. Denitrification potential rates decreased more than anammox potential rates with depth. The range in *ra* was 2.6–47.4% across stations, with an average of 34.2%. Excluding the 100 m and 930 m stations, *ra* was similar (i.e., ~40–47%) at stations with very different depths (120–3240 m), indicating that anammox and denitrification potential rates changed similarly with depth at these stations. As a proxy of organic C decomposition rates and therefore availability of labile C, we relied on NH_4^+ flux rates from porewater depth profiles and NH_4^+ production in

^{15}N incubations corresponding to the part of the incubation after NO_3^- had been consumed or in the case of the 3240 m station during the period that NO_3^- was present, as NO_3^- was never completely consumed during the incubation at the 3240 m station. In five out of seven stations, it was possible to compare trends in these two proxies, and the trends generally agreed at these five stations (100 m, 325 m, 940 m, 1460 m, and 3240 m), with highest NH_4^+ production at the two central shelf stations (Fig. 6B). NH_4^+ production rates in vials did not follow a consistent decrease with depth with similar rates across a depth range of 120–3240 m, with the exception in this depth range at the 325 m station.

3.4. Anammox specific 16S rRNA and hzo diversity and hzo gene abundance

A total of 112 clones were sequenced from seven 16S rRNA libraries, corresponding to each station. Based on BLAST and phylogenetic analyses, 30 16S rRNA sequences fell outside the anammox-specific cluster and were excluded from further analyses. The remaining 82 sequences had high identity with sequences in the *Candidatus* Scalindua group (Fig. 7). These sequences formed 19 OTUs at the 98% similarity level. A total of 112 *hzo* clones were also sequenced from seven libraries, corresponding to each station. All of the *hzo* sequences had high identity with Ca. Scalindua. The *hzo* nucleotide sequences formed 22 OTUs at the 96% similarity level.
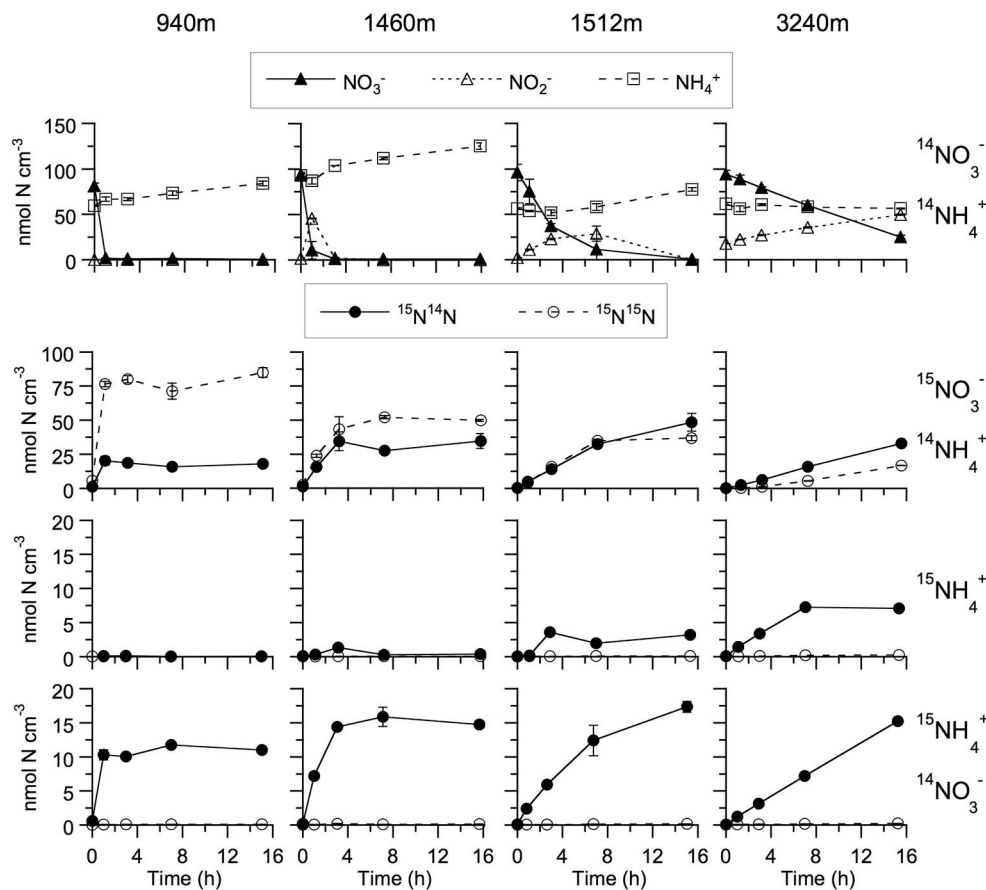
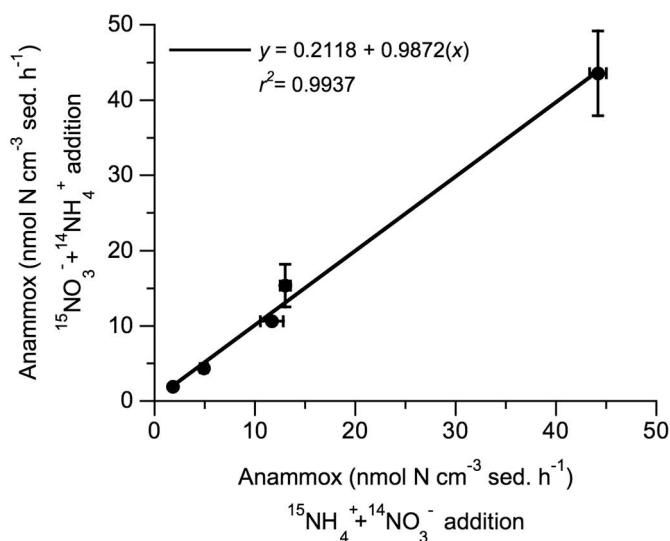**Fig. 4.** Same as in Fig. 3, except for the Peru margin slope and rise stations.

Fig. 5. Average (± SE, n = 3) anammox rates in homogenized sediments with added $^{15}NH_4^+ + {}^{14}NO_3^-$ (x-axis) or $^{15}NO_3^- + {}^{14}NH_4^+$ (y-axis) from five stations in the Peru margin. The mean slope of the line is not statistically different from one (p = 0.7954). Note: The two stations with visible evidence of *Thioploca* (i.e., 100 m and 325 m) are not shown, as anammox rates were determined with added $^{15}NH_4^+ + {}^{14}NO_3^-$ only due to the influence of intracellular NO_3^- during incubations in $^{15}NO_3^- + {}^{14}NH_4^+$ additions.

Eight OTUs were deduced from the Hzo amino acid sequences at the 99% similarity level. The two most abundant OTUs (PMHA-1 and PMHA-6) contained 92% of all sequenced clones in the same subcluster in phylogenetic trees (Fig. 8). Although these two sequence types differed by only one amino acid substitution, their relative abundance in clone libraries appeared related to water column depth, with PMHA-1 in greater abundance in shelf sediments than deeper stations, and the opposite trend for PMHA-6 (Fig. 6D). When aligned with the full-length Kuenenia sequence (CAJ71439), the change occurred at amino acid position 415, one residue from a putative heme binding motif, CDDCH at positions 416–420 (Schmid et al., 2008). The shallower station sequence (PMHA-1) has an alanine and the deeper station sequence (PMHA-6) has a valine at position 415.

The range in average *hzo* gene abundance across stations was 5.6×10^6–1.5×10^8 copies cm^{-3} sediment, with the lowest values at the deepest station (3240 m) and highest at the 325 m station (Table 3, Fig. 6A). The other five stations had similar average *hzo* abundance of about 5×10^7 copies cm^{-3} sediment. Average *hzo* gene abundance did not correlate significantly with potential anammox rates or *ra* across stations.

4. Discussion

4.1. Importance of denitrification and anammox as N loss pathways in marine sediments

In this study, rates of anammox and denitrification were determined in shipboard laboratory incubations of homogenized sediments with substrate concentrations that were not limiting. As such, the rates reported in this study are potential rates and therefore we have not extrapolated these rates to regional estimates of the total sediment N sink. Nevertheless, potential rates can be compared across studies that have used similar techniques to put the rates that we measured in perspective. The range of average denitrification potential rates (2.1–80.4 nmol N $cm^{-3} h^{-1}$) across stations that we measured is typical

Table 3
Potential rates (average $\pm$ standard deviation, n = 3) determined in shipboard ^{15}N incubations of homogenized sediments and *hzo* copy number.

Station	Depth (m)	Denitrif. (nmol N cm^{-3} h^{-1})	Anammox (nmol N cm^{-3} h^{-1})	*ra*	Dissolved NH$_4^+$ production (nmol N cm^{-3} h^{-1})	*hzo* (copies cm^{-3} × 10^7)
Shelf						
MC5	100	80.4 $\pm$ 3.8	2.2 $\pm$ 1.3	2.6 $\pm$ 1.6	9.5 $\pm$ 0.6	4.6 $\pm$ 0.7
MC2	120	67.6 $\pm$ 4.8	44.2 $\pm$ 1.5	39.6 $\pm$ 2.3	1.9 $\pm$ 0.8	6.6 $\pm$ 0.6
MC12	325	30.0 $\pm$ 6.5	25.1 $\pm$ 1.7	45.9 $\pm$ 7.1	6.9 $\pm$ 2.9	14.8 $\pm$ 3.7
Slope						
MC3	940	66.8 $\pm$ 2.9	13.0 $\pm$ 0.9	16.3 $\pm$ 0.8	1.3 $\pm$ 0.4	5.3 $\pm$ 0.7
MC4	1460	17.4 $\pm$ 3.4	11.7 $\pm$ 2.0	40.4 $\pm$ 8.8	1.7 $\pm$ 0.6	3.4[a]
MC9	1512	5.5 $\pm$ 1.0	5.0 $\pm$ 0.5	47.4 $\pm$ 7.2	2.3 $\pm$ 0.4	4.9 $\pm$ 0.2
Rise						
MC15	3240	2.1 $\pm$ 0.1	1.8 $\pm$ 0.1	47.2 $\pm$ 3.2	0.6 $\pm$ 0.1	0.6 $\pm$ 0.1

[a] n = 1 qPCR reaction for MC4, due to undetectable DNA template concentration in two out of three samples corresponding to this station.

for studies employing similar techniques at different locations in shelf or deep-sea sediments (Trimmer and Engström, 2011; Brin et al., 2014). Higher denitrification potential rates have been reported in samples from coastal bays or estuaries but in general the denitrification potential rates that we measured in shelf sediments are still in the range typically measured in shallower sub-tropical, temperate, or arctic sediments. Measurements of denitrification and anammox potential rates in sediments within ODZs are relatively rare, with one example from the Arabian Sea (Sokoll et al., 2012). Surprisingly, the average anammox potential rates that we measured at two of our shelf stations in the ODZ of 25.1 and 44.2 nmol N cm^{-3} h^{-1} (120 m and 325 m stations, respectively) are higher compared to the range of rates measured in different estuarine, shelf, or deep-sea sediments, including the Arabian Sea (Trimmer and Engström, 2011; Sokoll et al., 2012; Brin et al., 2014). The factors contributing to the high anammox potential rates that we measured are not clear but could be related to a combination of factors, including undetectable O$_2$ and relatively high NO$_3^-$ and NO$_2^-$ concentrations in the overlying water and lack of dense *Thioploca* at these two sites. Average anammox potential rates that we measured from the rest of the stations, including the shelf site with dense *Thioploca*, are in the range reported across other estuarine to deep-sea sediments.

In addition to determining denitrification and anammox potential rates using the type of ^{15}N incubations that we employed, rates of these two processes have been less commonly determined using porewater flux calculations or an intact core isotope pairing technique (Martin and Sayles, 2004; Trimmer et al., 2006; Trimmer and Engström, 2011). In deeper marine sediments (> 100 m water depth), incubations with homogenized sediments or whole cores have yielded similar results in terms of *ra* (Trimmer et al., 2013). Across eight stations in Washington Margin sediments with a water depth range of 2740–3110 m, the range in *ra* was 12–51% (average 38%) (Engström et al., 2009). In the North Sea, spanning a water depth of 50–2000 m, the range in *ra* was 15–65% (average 33%) (Trimmer and Nicholls, 2009). Across four stations in in the Arabian Sea with a water depth range of 360–1430 m, *ra* increased with depth from 7% to 40% (average ∼20%) (Sokoll et al., 2012). Average *ra* is similar among the Washington Margin, the North Sea, and our study, ∼33–38%, but higher than the average in the Arabian Sea. Comparing this relatively small dataset to rates in sediments from Skagerrak indicates that the relatively high *ra* of 79% in the Skagerrak is somewhat unusual, which could be due to relatively high levels of manganese oxides there, which could lead to manganese reducers outcompeting denitrifiers for organic carbon. This may give anammox bacteria a competitive advantage over denitrifiers for NO$_2^-$ at sites with high manganese oxides, in addition to low overall flux of labile organic carbon (Thamdrup and Dalsgaard, 2002; Engström et al., 2009). Our study indicates that overall anammox rates are likely to be quantitatively significant in Peru margin sediments, but not as high as denitrification rates, similar to other studies in deep sediments (Engström et al., 2009; Trimmer and Nicholls, 2009; Sokoll et al., 2012).

4.2. Methodological considerations

Applying the stable isotope pairing technique in sediments with *Thioploca* presents some challenges due to intracellular NO$_3^-$ and DNRA. Similarly, the presence of foraminifera could contribute intracellular NO$_3^-$ in our incubations (Glock et al., 2013). It should be noted that our application of the isotope pairing technique does not differentiate between bacterial or foraminiferal denitrification, but rather measures overall denitrification. Leakage or mixing of intracellular NO$_3^-$ into a pool of added ^{15}NO$_3^-$ can significantly reduce the atom% ^{15}N of NO$_3^-$ (F_n), leading to significant overestimates of anammox rates, if the effect of intracellular NO$_3^-$ on F_n is not taken into account (Song et al., 2013). In our study, we observed *Thioploca* at two stations (100 m and 325 m), which automatically indicated that intracellular NO$_3^-$ could be an issue. This was confirmed in porewater depth profiles with significantly higher NO$_3^-$ in the porewater than the bottom water, and ^{15}N incubations with high starting NO$_3^-$ concentrations. The F_n values that we calculated based on the standard approach by difference before and after ^{15}NO$_3^-$ addition were prone to very large error at these two stations. This resulted in negative anammox rates in some cases and highly variable estimates of *ra* among replicates using the standard equations of Thamdrup and Dalsgaard (2002) for ^{15}NO$_3^-$ + ^{14}NH$_4^+$ additions. To address this issue, others and we have used a modification of the standard isotope pairing equations (Sokoll et al., 2012; Song et al., 2013) relying on ^{15}NH$_4^+$ + ^{14}NO$_3^-$ additions instead of ^{15}NO$_3^-$ + ^{14}NH$_4^+$ additions to determine anammox rates, highlighting the importance of employing both combinations of isotopes (Song et al., 2013). In the other five stations where we did not observe *Thioploca*, anammox rates determined with either isotope combination treatment were similar across all five stations, indicating that intracellular NO$_3^-$ was not a significant factor in our results at these five stations.

A second potential issue with applying the stable isotope pairing technique in our samples is the influence of DNRA (Kartal et al., 2006; Song et al., 2016). If DNRA were taking place, ^{15}NH$_4^+$ would be produced from added ^{15}NO$_3^-$, potentially resulting in ^{15}N^{15}N production by anammox and an underestimate of anammox rates in incubations with added ^{15}NO$_3^-$ + ^{14}NH$_4^+$. This was not a factor at our two central shelf stations where we might expect the highest rates of DNRA, as anammox rates at these locations were determined in incubations with added ^{15}NH$_4^+$ + ^{14}NO$_3^-$, not added ^{15}NO$_3^-$ + ^{14}NH$_4^+$. However, DNRA could also influence the isotope labeling of the NH$_4^+$ pool with added ^{15}NH$_4^+$ + ^{14}NO$_3^-$ by diluting ^{15}NH$_4^+$ through conversion of ^{14}NO$_3^-$ to ^{14}NH$_4^+$. We accounted for potential dilution of ^{15}NH$_4^+$ during these incubations in our calculation of anammox rates by accounting for changes in the atom% of ^{15}N-NH$_4^+$ that may have occurred. Although we did not directly measure DNRA rates in this study, DNRA was not an issue in the determined anammox and denitrification
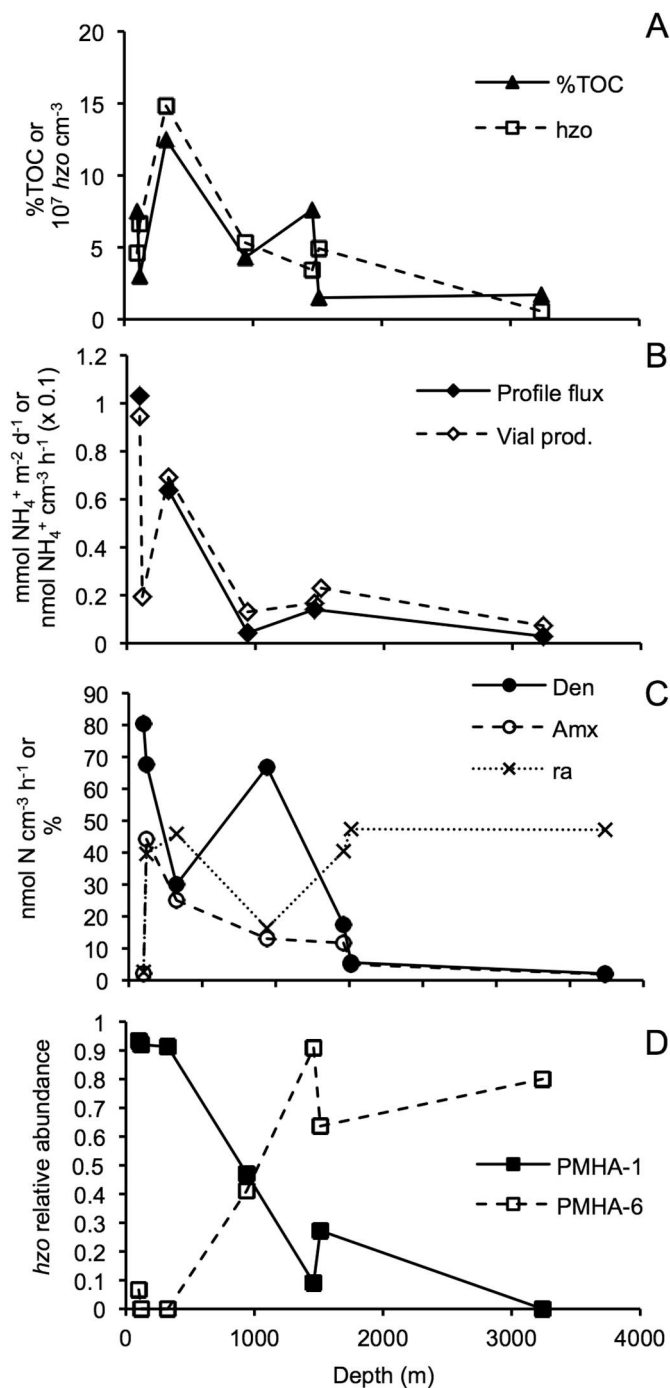
Fig. 6. Average of measured parameters and water column depth at each station in the study: (A) %TOC or qPCR *hzo* counts, (B) Upward NH_4^+ flux based on porewater depth profiles (mmol NH_4^+ m^{-2} d^{-1}) or dissolved NH_4^+ production rates measured in vial incubations, corresponding to NH_4^+ released during decomposition of organic matter (nmol NH_4^+ cm^{-3} h^{-1}), (C) anammox or denitrification potential rates (nmol N cm^{-3} h^{-1}) or *ra* (%), and (D) relative abundance of the two most abundant *hzo* genotypes in clone libraries.

rates at the five other stations, based on similar anammox rates between the two different combinations of isotope additions across these stations. Additional support for the estimated *ra* in shipboard incubations comes from the three stations where we were able to determine NO_3^- and NH_4^+ fluxes based on porewater profiles, as these estimates of *ra* were generally similar to those based on ^{15}N incubations. Directly measuring DNRA rates in these types of incubations would be important in future studies (Song et al., 2016).

4.3. Environmental controls on the relative contribution of anammox to rates

Thamdrup and Dalsgaard (2002) predicted a relationship of increasing *ra* with decreasing sediment organic C decomposition rates. However, the trend of decreasing organic C decomposition rates with depth can be variable, depending on the particular study region (e.g., Hedges and Keil, 1995). We could not use porewater oxygen profiles to assess organic C availability based on diffusive oxygen uptake rates across all the stations because three of the seven stations were in the oxygen deficient zone. We measured total organic carbon, but it did not correlate consistently with depth, although there were very high concentrations at the central two shelf stations, reflecting high organic matter deposition and burial in this area. As total organic carbon does not necessarily reflect labile carbon availability at the metabolic level (e.g., Hedges and Keil, 1995), we also examined NH_4^+ production rates as a proxy for organic C decomposition rates, and therefore organic C availability. NH_4^+ production rates were high at the two central shelf stations, indicating high organic C availability at these stations compared to the other five stations. In contrast, NH_4^+ production rates were generally similar at the other five stations, even though they varied widely with depth, suggesting lack of variability in organic C availability with depth in our other samples, which is not surprising given the large geographic area and varying topography over which we sampled.

Based on the original hypothesis by Thamdrup and Dalsgaard (2002), we would predict that *ra* should be lowest at the station with highest organic C decomposition rates, as indicated by NH_4^+ production rates. In agreement with their hypothesis, we found the lowest *ra* at the 100 m station, where NH_4^+ production rates were the highest. The next highest NH_4^+ production rates were at the 325 m station, while NH_4^+ production rates were relatively low at the rest of the stations. Based on relative differences in NH_4^+ production rates among stations, a second hypothesis based on Thamdrup and Dalsgaard (2002) would be that *ra* at the 325 m station would be closer to the low level measured at the 100 m station compared to the rest of the stations. Surprisingly, we did not find this pattern as the *ra* at the 325 m station was ~46%, similar to the other stations with relatively low NH_4^+ production. The jump in *ra* from the 100 m station to the 325 m station was due to both an increase in anammox potential rates and decrease in denitrification potential rates between these two stations. Denitrification potential rates did not show a consistent decrease with labile organic C, based on decreasing NH_4^+ production, suggesting that other factors in addition to labile organic C influenced our results.

Another factor controlling *ra* is likely to be NO_3^- availability. In sediments at different locations with similar labile organic C, greater NO_3^- concentrations in the overlying water or sediment porewater are related to greater *ra*, perhaps because of relieved competition for NO_2^- between denitrifying and anammox bacteria (Rich et al., 2008; Brin et al., 2014; Algar and Vallino, 2014). The visual presence of *Thioploca* at two stations in our study may have been a factor contributing to differences in NO_3^- availability in the sediments at these two stations due to the ability of *Thioploca* to transport NO_3^- down into sediments (Huettel et al., 1996). Zopfi et al. (2001) measured NO_3^- microprofiles in intact sediments with dense *Thioploca* mats, and found NO_3^- was not detectable in the porewater in the mat or underlying sediments, suggesting that *Thioploca* retain their intracellular NO_3^- stores efficiently. Porewater NO_3^- concentrations were somewhat higher in sediments with low density *Thioploca* compared to sediments with high density of *Thioploca* (Zopfi et al., 2001), suggesting that there could be differences in NO_3^- availability in sediments with different densities of *Thioploca* in our study. In turn, the density of *Thioploca* is likely related to labile organic C, as patterns of sulfide uptake in *Thioploca* suggest that these microbes are adapted to take advantage of periodically high sulfide concentrations following massive organic matter sedimentation events (Høgslund et al., 2009). Low density *Thioploca* at the 325 m station may
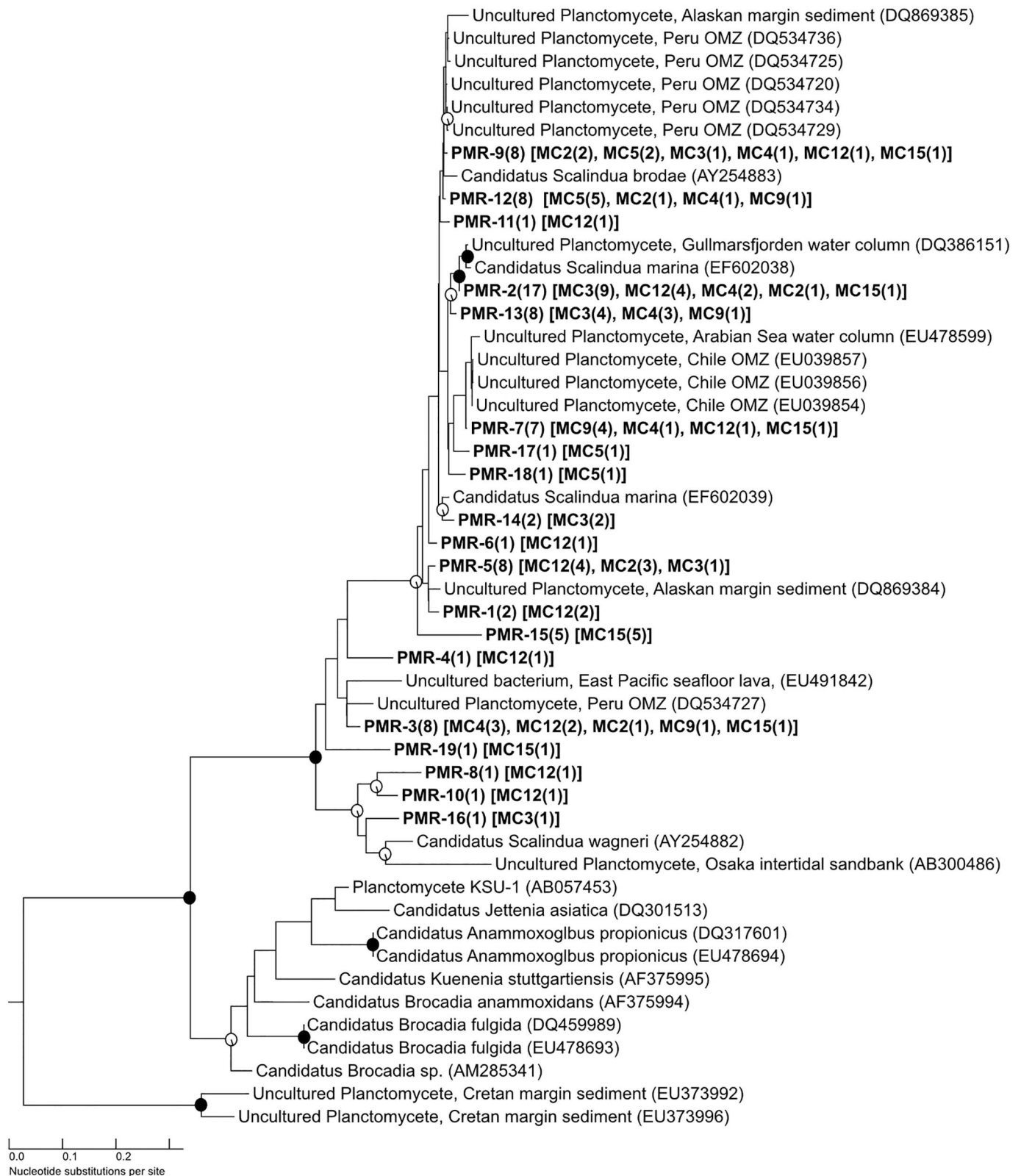
Fig. 7. Maximum-likelihood phylogenetic tree of 16S rRNA sequences. Sequences representing clone library OTUs from this study are bolded. Bolded leaf labels include the name of the OTU, the total number of clone sequences represented by that OTU in parentheses, followed by a list of what sites are represented within each OTU. The number of sequences per site is in parentheses. The tree was rooted with a 16S rDNA sequence from the Deltaproteobacterium *Desulfobulbus* sp. (GenBank: DSU85473). This outgroup was removed to improve branch length resolution. Scale bar units represent 0.1 nucleotide substitutions per site. Bootstrap support of > 70% (white circles) and > 90% (black circles) are shown.
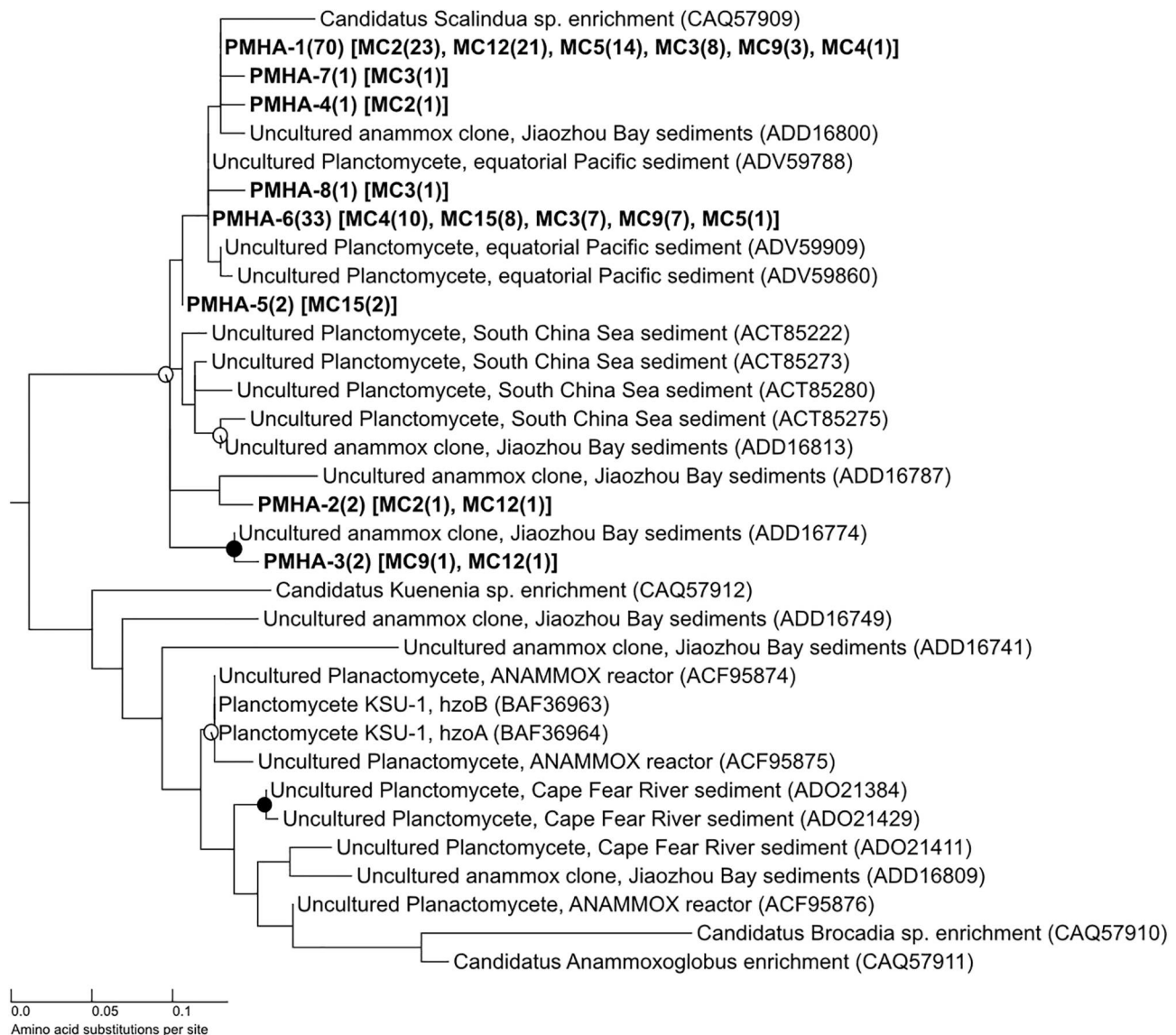
Fig. 8. Maximum-likelihood phylogenetic tree of Hzo amino acid sequences. Sequences representing OTUs from this study are bolded. Bolded labels include the name of the OTU, the total number of clone sequences represented by that OTU in parentheses, followed by a list of what stations are represented within each OTU, and the number of sequences per site. The tree was rooted with the Hzo group 2 sequence of Ca. Scalindua (GenBank: CAJ7180) as an outgroup (not shown). Scale bar units represent 0.05 amino acid substitutions per site. Bootstrap support of > 70% (white circles) and > 90% (black circles) are shown.

have been a remnant of a past organic matter sedimentation event at that location. Perhaps this could have led to greater NO_3^- leakage from *Thioploca* to the surrounding bacterial community in sediments at the 325 m station.

Our results of suppressed anammox rates in the *Thioploca* mat at the 100 m station do not necessarily contradict the results of Prokopenko et al. (2013), who found a close association between anammox bacteria and *Thioploca* and significant anammox rates at a station with *Thioploca* off Mexico. Few locations have been examined for the association between anammox and *Thioploca*, so the factors controlling the association are not well understood beyond Prokopenko et al. (2013). The *hzo* qPCR results from this study demonstrate that anammox bacteria were just as abundant at the 100 m station as some of the other stations, suggesting that anammox rates at the 100 m station were not limited by cell numbers of anammox bacteria but rather a physiological mechanism. Based on benthic fluxes and modeling in Peru margin sediments, Sommer et al. (2016) provided evidence that *Thioploca* strongly outcompete denitrifying and anammox bacteria for NO_3^- at locations with thick *Thioploca* mats and extremely high NH_4^+ production rates, much higher than

measured in our study. Bohlen et al. (2011) also sampled Peru margin sediments with *Thioploca* mats and NH_4^+ production rates more similar to our study. Based on Bohlen et al. (2011), anammox rates are completely inhibited in sediments with thick *Thioploca* mats, while denitrification rates are still active, which is a pattern similar to our results at the 100 m station. Inhibition of anammox rates due to hydrogen sulfide is also a possible factor (Jensen et al., 2008). However, *Thioploca* are proficient sulfur oxidizers and dissolved H_2S concentrations in intact *Thioploca* mats are generally below detection (Ferdelman et al., 1997), except in some extreme cases (Sommer et al., 2016). To rectify apparently contradictory results between our work and others in terms of the relationship between *Thioploca* and anammox, we propose that the relationship between anammox bacteria and *Thioploca* depends on the density and perhaps physiological condition of *Thioploca* found at a particular site, which would influence the ability of *Thioploca* to compete for NO_3^-. This might explain why we found relatively high rates of anammox in the presence of relatively sparse *Thioploca* at the 325 m station, but almost complete suppression of anammox rates at the 100 m station in the presence of a dense *Thioploca* mat.

4.4. Candidatus Scalindua in marine sediments

From deep sea hydrothermal vents (Byrne et al., 2008) to sediments collected across the equatorial Pacific (Hong et al., 2011), the dominance of Ca. Scalindua sequences is consistent in marine sediments. Anammox bacteria have been detected by 16S rDNA sequences in the water column in ODZs in the Eastern Pacific (Hamersley et al., 2007; Galán et al., 2009), the Arabian Sea (Jayakumar et al., 2009; Woebken et al., 2008), and the Namibian upwelling system (Kuypers et al., 2005). Sequences with high similarity to those of Ca. Scalindua also dominate these environments. Our study confirms low phylogenetic diversity of anammox bacteria in marine ecosystems (Schmid et al., 2007), with all anammox specific sequences forming a monophyletic cluster with representative sequences of Ca. Scalindua. Despite the pattern of dominance of Ca. Scalindua in the oceans, small-scale patterns of diversity within this group have been observed. Woebken et al. (2008) described two major clades of Ca. Scalindua in three major ODZs, with phylogenetic groupings (at 98% similarity for 16S rRNA genes) corresponding to different regions, i.e., Peru and the Arabian Sea. Hirsch et al. (2011) found supporting evidence for a deep-sea clade within Scalindua containing representatives from deep-sea hydrothermal vents and a submarine pyroclastic deposit. Spatial differentiation between anammox clades has also been observed at sites distributed across long distances in the equatorial Pacific (Hong et al. 2011).

In the Peru margin sediments, sequences from the sampling stations did not separate into site-specific phylogenetic subclusters, although the number of OTUs (defined at the 98% similarity for 16S rRNA and 96% similarity for *hzo*) exceeded the number of OTUs reported for the water column environments. A single amino acid change in the sequenced *hzo* fragments segregated the majority of the Peru margin anammox community into shelf and deep sediment types (Fig. 6D). While both of these types were part of the same subgroup within the larger Ca. Scalindua clade, this could be indicative of a microdiversity pattern that might be of ecological significance in terms of different physiological or kinetic adaptations to changes in pressure or temperature. Although we can only speculate on the functional implications of the amino acid change, examples of single amino acid changes resulting in differences in protein function are not uncommon (Bryan et al., 2000; Gong and Basilico, 1990; Joshi et al., 2000).

4.5. Conclusions

Results from our study suggest that anammox is a significant process contributing to N_2 production in Peru margin sediments, overall, with the exception of shallower shelf sediments with *Thioploca* mats. There are challenges to applying the standard isotope pairing technique in sediments with *Thioploca* due primarily to intracellular NO_3^- and possibly DNRA. Under these circumstances, our study further demonstrated the importance of parallel incubations with different combinations of isotopes to determine anammox and denitrification potential rates (Sokoll et al., 2012; Song et al., 2013). Except for the two central shelf stations, NH_4^+ production rates were similar in sediments with large differences in depth, indicative of overall high organic matter deposition in the region and large spatial variability over which we sampled. *ra* was relatively constant in four out of five stations with similar NH_4^+ production rates, consistent with the role of labile organic C flux as a factor controlling *ra*. In the two central shelf stations, with the highest NH_4^+ production rates, there were large differences in *ra* that were not expected based on NH_4^+ production rates alone. We propose that the difference in density of *Thioploca* and perhaps their physiological condition was a factor contributing to differences in *ra* at the two central shelf stations. The molecular data further support the ubiquitous role of anammox bacteria in the genus Ca. Scalindua in the marine environment, with an indication of fine-scale patterns in the distribution of diversity between shelf and deep sediments.

References

Algar, C., Vallino, J., 2014. Predicting microbial nitrate reduction pathways in coastal sediments. Aquat. Microb. Ecol. 71, 223–238. https://doi.org/10.3354/ame01678.

Babbin, A.R., Keil, R.G., Devol, A.H., Ward, B.B., 2014. Organic matter stoichiometry, flux, and oxygen control nitrogen loss in the ocean. Science 344, 406–408. https://doi.org/10.1126/science.1248364.

Berelson, W.M., Hammond, D.E., Oneill, D., Xu, X.M., Chin, C., Zukin, J., 1990. Benthic fluxes and pore water studies from sediments of the central equatorial North Pacific: nutrient diagenesis. Geochim. Cosmochim. Acta 54, 3001–3012.

Bohlen, L., Dale, A.W., Sommer, S., Mosch, T., Hensen, C., Noffke, A., et al., 2011. Benthic nitrogen cycling traversing the Peruvian oxygen minimum zone. Geochim. Cosmochim. Acta 75, 6094–6111.

Boudreau, B., 1997. Diagenetic Models and Their Implementation: Modelling Transport and Reactions in Aquatic Sediments. Springer, New York.

Braman, R.S., Hendrix, S.A., 1989. Nanogram nitrite and nitrate determination in environmental and biological materials by vanadium (III) reduction with chemiluminescence detection. Anal. Chem. 61, 2715–2718.

Brin, L.D., Giblin, A.E., Rich, J.J., 2014. Environmental controls on anammox and denitrification in Southern New England estuarine and shelf sediments. Limnol. Oceanogr. 59, 851–860.

Bristow, L.A., Dalsgaard, T., Tiano, L., Mills, D.B., Bertagnolli, A.D., Wright, J.J., et al., 2016. Ammonium and nitrite oxidation at nanomolar oxygen concentrations in oxygen minimum zone waters. Proc. Natl Acad. Sci. USA 113, 10601–10606. https://doi.org/10.1073/pnas.1600359113.

Broenkow, W.W., Cline, J.D., 1969. Colorimetric determination of dissolved oxygen at low concentrations. Limnol. Oceanogr. 14, 450–454.

Bryan, G.T., Wu, K.-S., Farrall, L., Jia, Y., Hershey, H.P., McAdams, S.A., et al., 2000. A single amino acid difference distinguishes resistant and susceptible alleles of the rice blast resistance gene Pi-ta. Plant Cell Online 12, 2033–2046.

Byrne, N., Strous, M., Crepeau, V., Kartal, B., Birrien, J.-L., Schmid, M., et al., 2008. Presence and activity of anaerobic ammonium-oxidizing bacteria at deep-sea hydrothermal vents. ISME J 3, 117–123.

Christensen, J.P., Murray, J.W., Devol, A.H., Codispoti, L.A., 1987. Denitrification in continental shelf sediments has major impact on the oceanic nitrogen budget. Glob. Biogeochem. Cycles 1, 97–116.

Dalsgaard, T., Thamdrup, B., Farías, L., Peter Revsbech, N., 2012. Anammox and denitrification in the oxygen minimum zone of the eastern South Pacific. Limnol. Oceanogr. 57, 1331–1346. https://doi.org/10.4319/lo.2012.57.5.1331.

Desantis, T.Z., Hugenholtz, P., Larsen, N., Rojas, M., Brodie, E.L., Keller, K., et al., 2006. Greengenes, a chimera-checked 16S rRNA gene database and workbench compatible with ARB. Appl. Environ. Microbiol. 72, 5069–5072.

Devol, A.H., 1991. Direct measurement of nitrogen gas fluxes from continental shelf sediments. Nature 349, 319–321.

Engström, P., Dalsgaard, T., Hulth, S., Aller, R.C., 2005. Anaerobic ammonium oxidation by nitrite (anammox): implications for N2 production in coastal marine sediments. Geochim. Cosmochim. Acta 69, 2057–2065.

Engström, P., Penton, C.R., Devol, A.H., 2009. Anaerobic ammonium oxidation in deep-sea sediments off the Washington margin. Limnol. Oceanogr. 54, 1643–1652.

Ferdelman, T.G., Lee, C., Pantoja, S., Harder, J., Bebout, B.M., Fossing, H., 1997. Sulfate reduction and methanogenesis in a *Thioploca*-dominated sediment off the coast of Chile. Geochim. Cosmochim. Acta 61, 3065–3079.

Fossing, H., Gallardo, V.A., Jorgensen, B.B., Huttel, M., Nielsen, L.P., Schulz, H., et al., 1995. Concentration and transport of nitrate by the mat-forming sulfur bacterium *Thioploca*. Nature 374, 713–715.

Froelich, P.N., Arthur, M.A., Burnett, W.C., Deakin, M., Hensley, V., Jahnke, R., et al., 1988. Early diagenesis of organic matter in Peru continental margin sediments: phosphorite precipitation. Mar. Geol. 80, 309–343.

Galán, A., Molina, V., Thamdrup, B., Woebken, D., Lavik, G., Kuypers, M.M.M., et al., 2009. Anammox bacteria and the anaerobic oxidation of ammonium in the oxygen minimum zone off northern Chile. Deep Sea Res. Part II Top. Stud. Oceanogr. 56, 1021–1031.

Galloway, J.N., Dentener, F.J., Capone, D.G., Boyer, E.W., Howarth, R.W., Seitzinger, S.P., et al., 2004. Nitrogen cycles: past, present, and future. Biogeochemistry 70, 153–226.

Glock, N., Schönfeld, J., Eisenhauer, A., Hensen, C., Mallon, J., Sommer, S., 2013. The role of benthic foraminifera in the benthic nitrogen cycle of the Peruvian oxygen minimum zone. Biogeosciences 10, 4767–4783. https://doi.org/10.5194/bg-10-4767-2013.

Gong, S.S., Basilico, C., 1990. A mammalian temperature-sensitive mutation affecting G1 progression results from a single amino acid substitution in asparagine synthetase.

Nucleic Acids Res. 18, 3509.

Guindon, S., Dufayard, J., Lefort, V., Anisimova, M., Hordijk, W., Gascuel, O., 2010. New algorithms and methods to estimate maximum-likelihood phylogenies: assessing the performance of PhyML 3.0. Syst. Biol. 59, 307–321.

Haeckel, M., Konig, I., Reich, V., Weber, M.E., Suess, E., 2001. Pore water profiles and numerical modelling of biogeochemical processes in Peru Basin deep-sea sediments. Deep. Res. Part II-Topical Stud. Oceanogr. 48, 3713–3736.

Hamersley, M.R., Lavik, G., Woebken, D., Rattray, J.E., Lam, P., Hopmans, E.C., et al., 2007. Anaerobic ammonium oxidation in the Peruvian oxygen minimum zone. Limnol. Oceanogr. 52, 923–933.

Hedges, J.I., Keil, R.G., 1995. Sedimentary organic-matter preservation: an assessment and speculative synthesis. Mar. Chem. 49, 81–115.

Henrichs, S.M., Farrington, J.W., 1984. Peru upwelling region sediments near 15-degrees south. 1. Remineralization and accumulation of organic matter. Limnol. Oceanogr. 29, 1–19.

Hirsch, M.D., Long, Z.T., Song, B., 2011. Anammox bacterial diversity in various aquatic ecosystems based on the detection of hydrazine oxidase genes. Microb. Ecol. 61, 264–276.

Høgslund, S., Revsbech, N.P., Kuenen, J.G., Jørgensen, B.B., Gallardo, V.A., van de Vossenberg, J., et al., 2009. Physiology and behaviour of marine *Thioploca*. ISME J. 3, 647–657. https://doi.org/10.1038/ismej.2009.17.

Hong, Y.-G., Yin, B., Zheng, T.-L., 2011. Diversity and abundance of anammox bacterial community in the deep-ocean surface sediment from equatorial Pacific. Appl. Microbiol. Biotechnol. 89, 1233–1241. https://doi.org/10.1007/s00253-010-2925-4.

Huettel, M., Forster, S., Kloser, S., Fossing, H., 1996. Vertical migration in the sediment-dwelling sulfur bacteria *Thioploca* spp in overcoming diffusion limitations. Appl. Environ. Microbiol. 62, 1863–1872.

Jayakumar, A., Naqvi, S.W.A., Ward, B.B., 2009. Distribution and relative quantification of key genes involved in fixed nitrogen loss from the Arabian Sea oxygen minimum zone. In: Wiggert, J.D., Hood, R.R. (Eds.), Indian Ocean Biogeochemical Processes and Ecological Variability. American Geophysical Union, Washington, D, C, pp. 187–203.

Jensen, M.M., Kuypers, M., Lavik, G., Thamdrup, B., 2008. Rates and regulation of anaerobic ammonium oxidation and denitrification in the Black Sea. Limnol. Oceanogr. 53, 23–36.

Joshi, M.D., Sidhu, G., Pot, I., Brayer, G.D., Withers, S.G., McIntosh, L.P., 2000. Hydrogen bonding and catalysis: a novel explanation for how a single amino acid substitution can change the pH optimum of a glycosidase. J. Mol. Biol. 299, 255–279.

Kartal, B., Keltjens, J.T., 2016. Anammox biochemistry : a tale of Heme c proteins. Trends Biochem. Sci. 41, 998–1011. https://doi.org/10.1016/j.tibs.2016.08.015.

Kartal, B., Kuypers, M.M.M., Lavik, G., Schalk, J., den Camp, H., Jetten, M.S.M., et al., 2006. Anammox bacteria disguised as denitrifiers: nitrate reduction to dinitrogen gas via nitrite and ammonium. Environ. Microbiol. 9, 635–642.

Kartal, B., Keltjens, J.T., Jetten, M.S.M., 2011a. Metabolism and genomics of anammox bacteria. In: Ward, B.B., Arp, D.J., Klotz, M.G. (Eds.), Nitrification. American Society for Microbiology Press, Washington, D, C, pp. 181–200.

Kartal, B., Maalcke, W.J., de Almeida, N.M., Cirpus, I., Gloerich, J., Geerts, W., et al., 2011b. Molecular mechanism of anaerobic ammonium oxidation. Nature 479, 127–130.

Klotz, M.G., Schmid, M.C., Strous, M., op den Camp, H.J.M., Jetten, M.S.M., Hooper, A.B., 2008. Evolution of an octahaem cytochrome c protein family that is key to aerobic and anaerobic ammonia oxidation by bacteria. Environ. Microbiol. 10, 3150–3163. https://doi.org/10.1111/j.1462-2920.2008.01733.x.

Koroleff, F., 1983. Determination of nutrients. In: Grasshoff, K. (Ed.), Methods of Seawater Analysis. Verlag Chemie.

Kuypers, M.M.M., Sliekers, A.O., Lavik, G., Schmid, M., Jørgensen, B.B., Kuenen, J.G., et al., 2003. Anaerobic ammonium oxidation by anammox bacteria in the Black Sea. Nature 422, 608–611.

Kuypers, M.M.M., Lavik, G., Woebken, D., Schmid, M., Fuchs, B.M., Amann, R., et al., 2005. Massive nitrogen loss from the Benguela upwelling system through anaerobic ammonium oxidation. Proc. Natl. Acad. Sci. U. S. A. 102, 6478–6483.

Lam, P., Lavik, G., Jensen, M.M., van de Vossenberg, J., Schmid, M., Woebken, D., et al., 2009. Revising the nitrogen cycle in the Peruvian oxygen minimum zone. Proc. Natl. Acad. Sci. U. S. A. 106, 4752–4757. https://doi.org/10.1073/pnas.0812444106.

Levin, L., Gutierrez, D., Rathburn, A., Neira, C., Sellanes, J., Munoz, P., et al., 2002. Benthic processes on the Peru margin: a transect across the oxygen minimum zone during the 1997–98 El Niño. Prog. Oceanogr. 53, 1–27.

Martin, W.R., Sayles, F.L., 2004. Organic matter cycling in sediments of the continental margin in the northwest Atlantic Ocean. Deep Sea Res. Part I Oceanogr. Res. Pap. 51, 457–489.

Middelburg, J.J., Soetaert, K., Herman, P.M.J., Heip, C.H.R., 1996. Denitrification in marine sediments: a model study. Glob. Biogeochem. Cycles 10, 661–673.

Neef, A., Amann, R., Schlesner, H., Schleifer, K.H., 1998. Monitoring a widespread bacterial group: in situ detection of planctomycets with 16S rRNA-targeted probes. Microbiology 144, 3257–3266.

Nielsen, L.P., 1992. Denitrification in sediment determined from nitrogen isotope pairing. FEMS Microbiol. Ecol. 86, 357–362.

Otte, S., Kuenen, J.G., Nielsen, L.P., Paerl, H.W., Zopfi, J., Schulz, H.N., et al., 1999. Nitrogen, carbon, and sulfur metabolism in natural *Thioploca* samples. Appl. Environ. Microbiol. 65, 3148–3157.

Prokopenko, M.G., Hirst, M.B., De Brabandere, L., Lawrence, D.J.P., Berelson, W.M., Granger, J., et al., 2013. Nitrogen losses in anoxic marine sediments driven by

Thioploca-anammox bacterial consortia. Nature 500, 194–198.

Rich, J.J., Dale, O.R., Song, B., Ward, B.B., 2008. Anaerobic ammonium oxidation (anammox) in Chesapeake Bay sediments. Microb. Ecol. 55, 311–320.

Risgaard-Petersen, N., Meyer, R.L., Schmid, M., Jetten, M.S.M., Enrich-Prast, A., Rysgaard, S., et al., 2004. Anaerobic ammonium oxidation in an estuarine sediment. Aquat. Microb. Ecol. 36, 293–304.

Risgaard-Petersen, N., Langezaal, A.M., Ingvardsen, S., Schmid, M.C., Jetten, M.S.M., Op den Camp, H.J.M., et al., 2006. Evidence for complete denitrification in a benthic foraminifer. Nature 443, 93–96. https://doi.org/10.1038/nature05070.

Rozen, S., Skaletsky, H., 1999. Primer3 on the WWW for general users and for biologist programmers. Methods Mol. Biol. 132, 365–386.

Schloss, P.D., Westcott, S.L., Ryabin, T., Hall, J.R., Hartmann, M., Hollister, E.B., et al., 2009. Introducing mothur: open-source, platform-independent, community-supported software for describing and comparing microbial communities. Appl. Environ. Microbiol. 75, 7537–7541.

Schmid, M.C., Maas, B., Dapena, A., de Pas-Schoonen, K.V., de Vossenberg, J.V., Kartal, B., et al., 2005. Biomarkers for in situ detection of anaerobic ammonium-oxidizing (anammox) bacteria. Appl. Environ. Microbiol. 71, 1677–1684.

Schmid, M.C., Risgaard-Petersen, N., van de Vossenberg, J., Kuypers, M.M.M., Lavik, G., Petersen, J., et al., 2007. Anaerobic ammonium-oxidizing bacteria in marine environments: widespread occurrence but low diversity. Environ. Microbiol. 9, 1476–1484.

Schmid, M.C., Hooper, A.B., Klotz, M.G., Woebken, D., Lam, P., Kuypers, M.M.M., et al., 2008. Environmental detection of octahaem cytochrome c hydroxylamine/hydrazine oxidoreductase genes of aerobic and anaerobic ammonium-oxidizing bacteria. Environ. Microbiol. 10, 3140–3149.

Schulz, H.N., Jorgensen, B.B., Fossing, H.A., Ramsing, N.B., 1996. Community structure of filamentous, sheath-building sulfur bacteria, *Thioploca* spp, off the coast of Chile. Appl. Environ. Microbiol. 62, 1855–1862.

Sokoll, S., Holtappels, M., Lam, P., Collins, G., Schlüter, M., Lavik, G., et al., 2012. Benthic nitrogen loss in the Arabian Sea off Pakistan. Front. Microbiol. 3, 1–17. https://doi.org/10.3389/fmicb.2012.00395.

Sommer, S., Gier, J., Treude, T., Lomnitz, U., Dengler, M., Cardich, J., et al., 2016. Depletion of oxygen, nitrate and nitrite in the Peruvian oxygen minimum zone cause an imbalance of benthic nitrogen fluxes. Deep. Res. Part I 112, 113–122. https://doi.org/10.1016/j.dsr.2016.03.001.

Song, G.D., Liu, S.M., Marchant, H., Kuypers, M.M.M., Lavik, G., 2013. Anammox, denitrification and dissimilatory nitrate reduction to ammonium in the East China Sea sediment. Biogeosciences 10, 6851–6864. https://doi.org/10.5194/bg-10-6851-2013.

Song, G.D., Liu, S.M., Kuypers, M.M.M., Lavik, G., 2016. Application of the isotope pairing technique in sediments where anammox, denitrification, and dissimilatory nitrate reduction to ammonium coexist. Limnol. Oceanogr. Methods 14, 801–815. https://doi.org/10.1002/lom3.10127.

Sonthiphand, P., Hall, M.W., Neufeld, J.D., 2014. Biogeography of anaerobic ammonia-oxidizing (anammox) bacteria. Front. Microbiol. 5, 1–14. https://doi.org/10.3389/fmicb.2014.00399.

Strickland, J.D., Parsons, T.R., 1972. A practical handbook of seawater analysis. Fish. Res. board Canada 167, 1–311.

Thamdrup, B., Canfield, D.E., 1996. Pathways of carbon oxidation in continental margin sediments off Central Chile. Limnol. Oceanogr. 41, 1629–1650.

Thamdrup, B., Dalsgaard, T., 2000. The fate of ammonium in anoxic manganese oxide-rich marine sediment. Geochim. Cosmochim. Acta 64, 4157–4164.

Thamdrup, B., Dalsgaard, T., 2002. Production of N_2 through anaerobic ammonium oxidation coupled to nitrate reduction in marine sediments. Appl. Environ. Microbiol. 68, 1312–1318.

Trimmer, M., Engström, P., 2011. Distribution, activity, and ecology of anammox bacteria in aquatic environments. In: Ward, B.B., Arp, D.J., Klotz, M.G. (Eds.), Nitrification. American Society for Microbiology Press, Washington, D, C, pp. 201–235.

Trimmer, M., Nicholls, J.C., 2009. Production of nitrogen gas via anammox and denitrification in intact sediment cores along a continental shelf to slope transect in the North Atlantic. Limnol. Oceanogr. 54, 577–589.

Trimmer, M., Risgaard-Petersen, N., Nicholls, J.C., Engström, P., 2006. Direct measurement of anaerobic ammonium oxidation (anammox) and denitrification in intact sediment cores. Mar. Ecol. Prog. Ser. 326, 37–47.

Trimmer, M., Engström, P., Thamdrup, B., Trimmer, M., Engström, P., 2013. Stark contrast in denitrification and Anammox across the deep Norwegian trench in the Skagerrak. Appl. Environ. Microbiol. 79, 7381–7389. https://doi.org/10.1128/AEM.01970-13.

Ullman, W.J., Aller, R.C., 1982. Diffusion-coefficients in nearshore marine-sediments. Limnol. Oceanogr. 27, 552–556.

Ward, B.B., Devol, A.H., Rich, J.J., Chang, B.X., Bulow, S.E., Naik, H., et al., 2009. Denitrification as the dominant nitrogen loss process in the Arabian Sea. Nature 461, 78–81.

Woebken, D., Lam, P., Kuypers, M.M.M., Naqvi, S.W.A., Kartal, B., Strous, M., et al., 2008. A microdiversity study of anammox bacteria reveals a novel Candidatus Scalindua phylotype in marine oxygen minimum zones. Environ. Microbiol. 10, 3106–3119.

Zopfi, J., Kjaer, T., Nielsen, L.P., Jorgensen, B.B., 2001. Ecology of *Thioploca* spp.: nitrate and sulfur storage in relation to chemical microgradients and influence of *Thioploca* spp. on the sedimentary nitrogen cycle. Appl. Environ. Microbiol. 67, 5530–5537.

Zumft, W.G., 1997. Cell biology and molecular basis of denitrification. Microbiol. Mol. Biol. Rev. 61, 533–616.